Emergence of Diverse Structures and Functions from a State Transition Function Facilitating Origin and Replication of the Byl Replicator.

Perry W. Swanborough

Abstract

Replication of the John Byl cellular automata replicator (1989) and its origin from an isolated cell in an oriented state requires 183 explicit state transition rules, but the corresponding state-set inclusive of eight unoriented active states {1,2,3,4,5,L,E,F} and one oriented active state (^) prescribes a vast number of possible state transition functions supporting the replicator and its origin, each containing 93,262 explicit state transition rules. The particular state transition function supporting the origin and replication of the replicator, with all other 93,262 – 183 = 93,079 rules prescribing state conservation (neighbourhood CNESW - - > C´ = C), supports the appearance and development of structures and functions additional to appearance and replication of replicator structures. For abiogenesis, these results suggest the possibility that interactions of ancient replicators with each other and with coexisting persistent structures enabled the subsequent appearance of containment (membranes), metabolism and information processing, thereby founding ancestral life.

Keywords: abiogenesis, Byl replicator, cellular automata, definitions of life, loop replicator

Introduction

In reference [7], it was supposed that implementation of a wide range of biologically-meaningful structures and functions might not be possible by the interactions of loop replicators in cellular automata (CA) environments, given the algorithmic rigidity of the replicators and spatial rigidity of their subsequent colonies. In that study, the generic loop replicator exemplified by Christopher Langton [3] and simplified by John Byl [1] was represented by a single cell in an oriented state with a comprehensive set of state transition rules facilitating a wide range of dynamic behaviour and structures. In this new study, I have rethought the question of what can emerge from interactions of instances of CA loop replicators, but this time without any requirements for simplification of the structural or state transition function details.

A CA state transition function is a set of state transition rules implementing the change of cell state C at time t to the state C´ at time t+1. A von Neumann state transition rule is described as CNESW → C´ where **CNESW** (cell states at **C**entre, **N**orth, **E**ast, **S**outh and **W**est cells) defines a von Neumann CA neighbourhood within a two-dimensional grid. There are 143 explicit state-transition rules facilitating replication of an established replicator [1] with an additional 40 rules required for origin of a Byl replicator from a single isolated cell in the oriented state **^** [6] giving a total of 183 explicit state transition rules facilitating origin and replication. Given a quiescent state 0, eight unoriented active states {1,2,3,4,5,L,E,F} and one oriented active state **^** (with rotated equivalents **<**, **v** and **>**) in the state set underlying the comprehensive origin-plus-replication state transition function, there are 93,262 distinct von Neumann neighbourhoods and therefore 93,262 state transition rules in any specific comprehensive state transition function. Given 93,262 CNESW neighbourhoods and a choice from 13 state transitions (C → C´) assignable for each, there are 183 + 13^(93,262-183) definable state transition functions supporting origin and replication of the Byl replicator.

What phenomena beyond replication are possible in application of a comprehensive state transition function of 93,262 rules? Two convenient C → C´ rule categories for all 93,262-183 = 93,079 other von Neumann neighbourhoods are CNESW → C´ = 0 (state C transitions to quiescent) or CNESW → C

(C′ = C, *i.e.* cell states are maintained by default until an applicable state transition rule determines a change of state). Incorporating the latter defines a state transition function which not only supports the appearance and replication of replicator structures, but facilitates the appearance of additional structures and functions.

Methods

A state transition function facilitating the origin and replication of the Byl replicator was applied to random distributions of cell states across a 180 x 180 cell grid for the purpose of detecting the emergence of any interesting dynamics and structures additional to the appearance and replication of Byl replicators. The probability density at which the active states were assigned was set to 0.005. All graphics were produced with *Processing* software [5] with the states to colours mapping shown in Table 1.

Table 1. In all images shown in the figures, cell states are represented by colours as shown.

State:	0 (quiescent)	1	2	3	4	5	{L, E, F, **^**,**<**,**v**,**>**}
Colour:	black	red	blue	pink	green	yellow	white

The left panel of Figure 1 below shows an initial (Time = 0) 180 x 180 cell field of randomly-distributed active cell states from the set {1,2,3,4,5,L,E,F,**^**,**<**,**v**,**>**} in a background of quiescent state 0 (black) and outer perimeter of state 2 (blue). The right-hand panel of Figure 1 shows the development of the field at Time = 50 by application of the state-transition function. The applied state transition rules corresponding to CNESW neighbourhoods not represented in the origin and replication state transition function were eliminative, *i.e.* CNESW → C′ = 0 (reversion to quiescence). Development of the initial field at Time = 50 is shown also in Figure 2, but in this case with state-conserving transition rules corresponding to CNESW neighbourhoods not represented in the Byl origin and replication state transition function, *i.e.* CNESW → C′ = C.

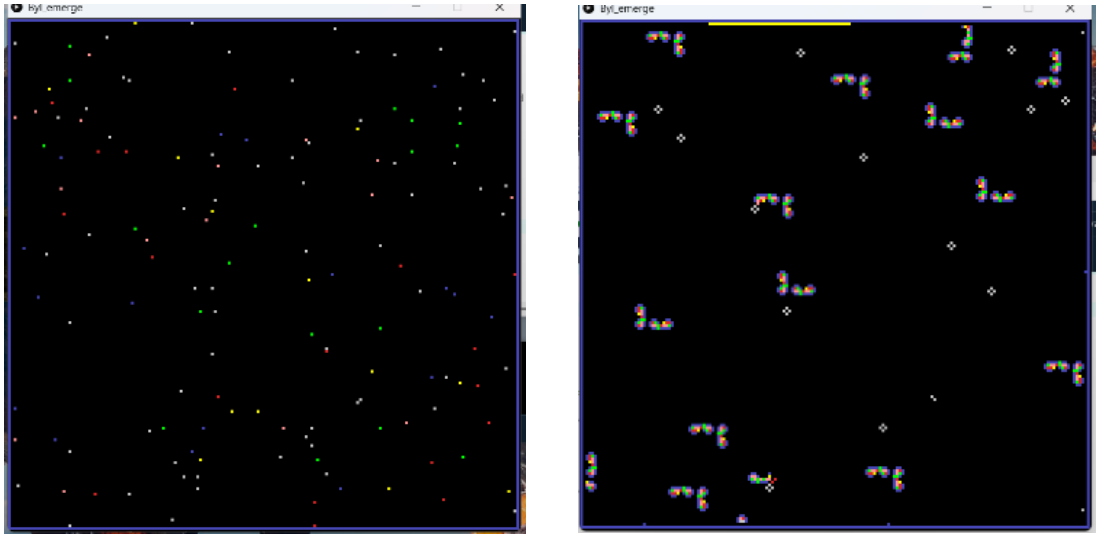

Figure 1. Development of a field of randomly-distributed active cell states from initialisation (left, Time = 0), to Time = 50 (right) by application of the Byl state transition function facilitating origin of replicators from states {**^**, **<**, **v**, **>**} and replication of consequent instances of the replicator structure. The state transition rules applying to CNESW neighbourhoods not corresponding to any explicitly-defined rules for replicator origin and replication force reversion to quiescence, *i.e.* cell state C at time t reverts to state 0 at time t+1 (CNESW → C′ = 0).

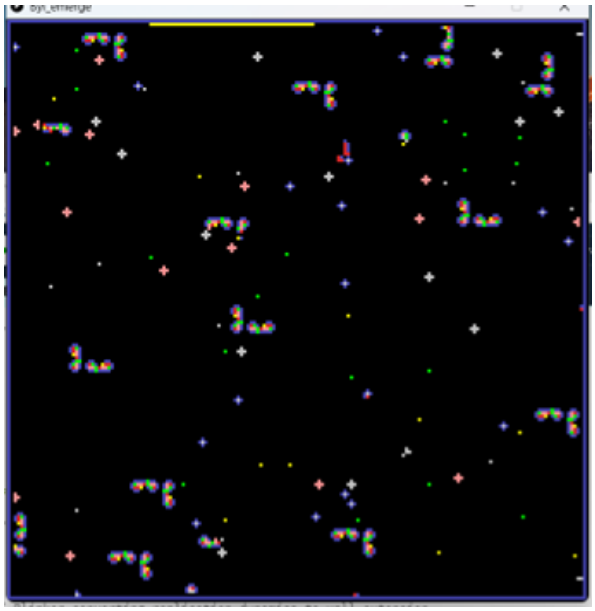

Figure 2. An alternative development of the Time = 0 field shown in Figure 1. This frame (Time = 50) is directly comparable to the right-hand panel in Figure 1, but in this case the state transition rules applying to neighbourhoods not corresponding to any explicitly-defined rules for replicator origin and replication are conservative, *i.e.* state C at time t is unchanged at time t+1 (CNESW → C′ = C).

Comparison of Figure 2 with the right-hand panel of Figure 1 indicates that assigning state-conserving transition rules CNESW → C′ = C to neighbourhoods not represented in the explicit origin-and-replication state transition rules facilitates a wider range of persistent non-quiescent structures than for the case in Figure 1 where default state transition C → 0 (quiescence) applies. Therefore,

investigation of the CA environment equipped with the state transition function incorporating the state-conserving transition rules was indicated and explored.

Several replications of development from random initial distributions of active cell states were run in *Processing* [5], revealing some interesting emergent structures and dynamic behaviour. CA fields were subsequently organised to reproduce some of the observed structures and developments of interest without the presence of irrelevant and interfering activity, and results were captured in screenshots subsequently cropped to display the dynamics of interest.

Results

Notable structures and dynamics were captured in screenshots cropped for display in Figures 3 to 10 below. Figure 3 shows the interaction of two vertically-opposed Byl replicators causing the horizontal extension of spatially- and temporally-periodic arms to both the east and west. At Time = 12 (first frame), the replicators in their respective normal replication cycles have not yet interacted, but at Time 13 the first interaction step diverting normal isolated replication has occurred. From Time 14 to 25 horizontally extending arms have initiated. The last frame (Time = 50) shows the result of regular extension of the arms (note that in the direction of extension, the state 2 (blue) layer of the arms is the rightmost layer). The small period-4 oscillator west (left) of the westward extending arm influences it in an interesting way when it arrives for the inevitable interaction and consequent development, shown in Figure 4.

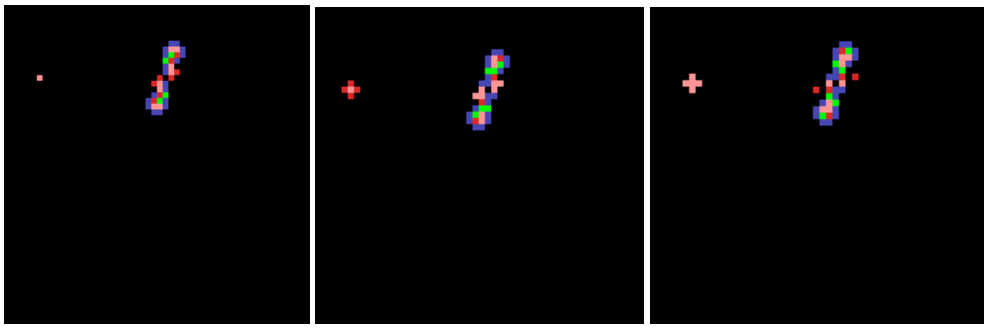

Time =12 Time = 13 Time = 14

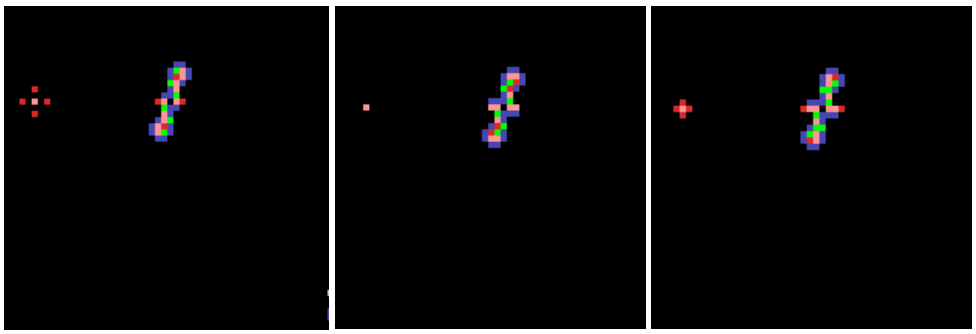

Time = 15 Time = 16 Time = 17

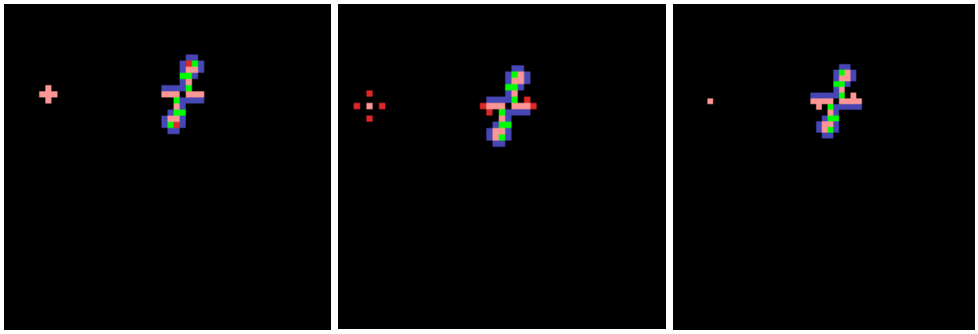

Time = 18 Time = 19 Time = 20

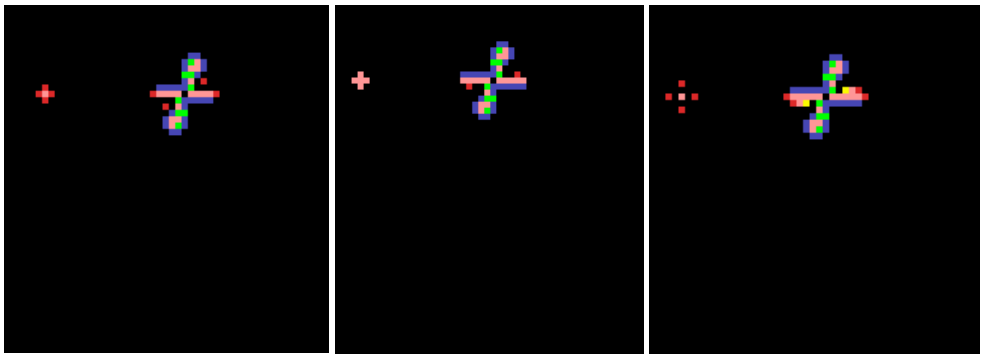

Time = 21 Time = 22 Time = 23

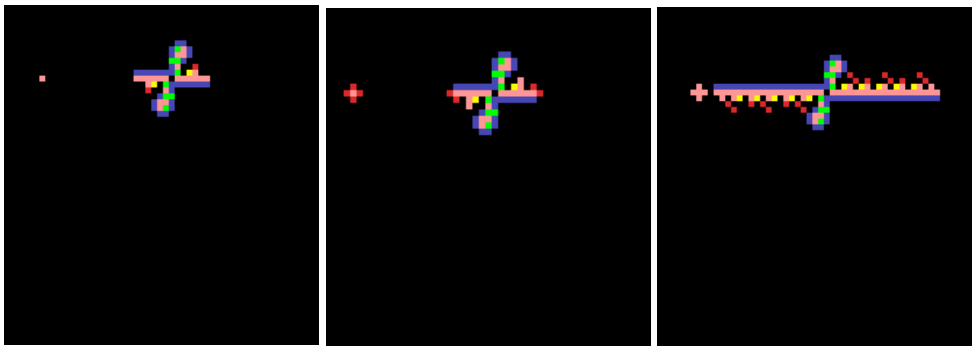

Time = 24 Time = 25 … …Time = 50

Figure 3. The interaction of two vertically-opposed replicators originating at Time = 0 from isolated cells in states **>** (north) and **<** (south) causes the horizontal extension of spatially- and temporally-periodic arms to both the east and west. By Time = 50, interaction of the westward arm with a period-4 oscillator is imminent.

The sequence shown in Figure 3 is continued below in Figure 4 to show the consequence of the westward-extending arm interacting with the oscillator. A modified form of arm (a dynamically-uniform band of three states) continues west as the preceding arm is redirected south. The last frame (Time = 90) shows extension of the two arms by a considerable distance.

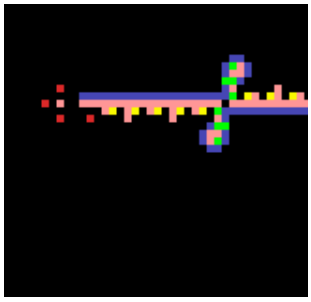

Time = 51

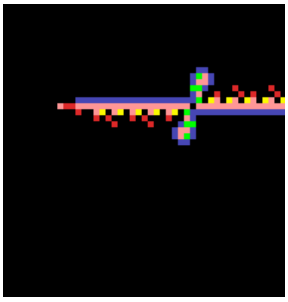

Time = 52

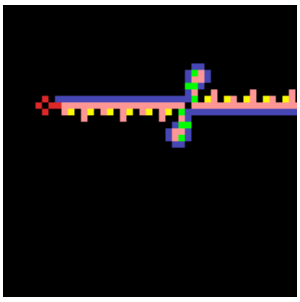

Time = 53

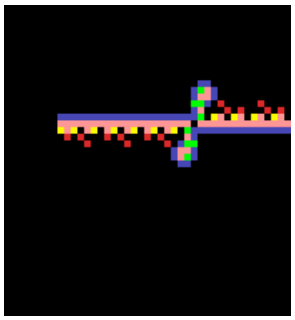

Time = 54

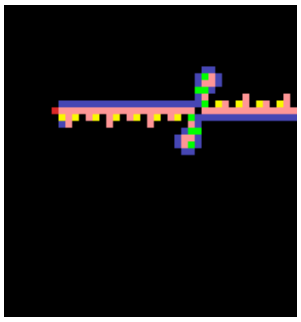

Time = 55

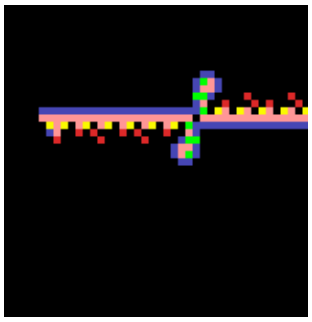

Time = 56

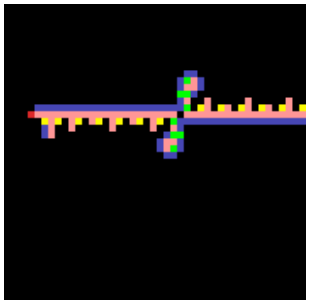

Time = 57

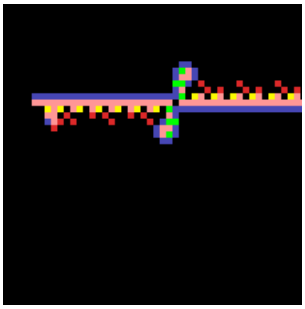

Time = 58

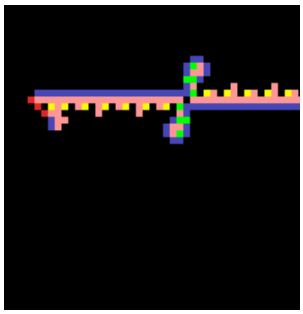

Time = 59

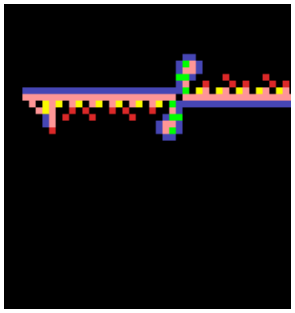

Time = 60

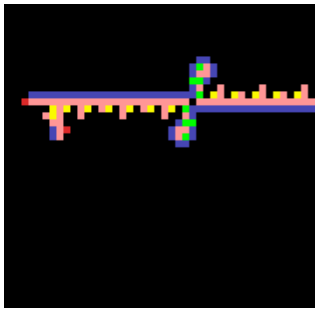

Time = 61

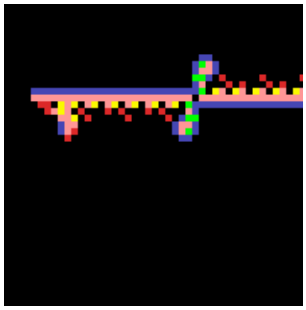

Time = 62

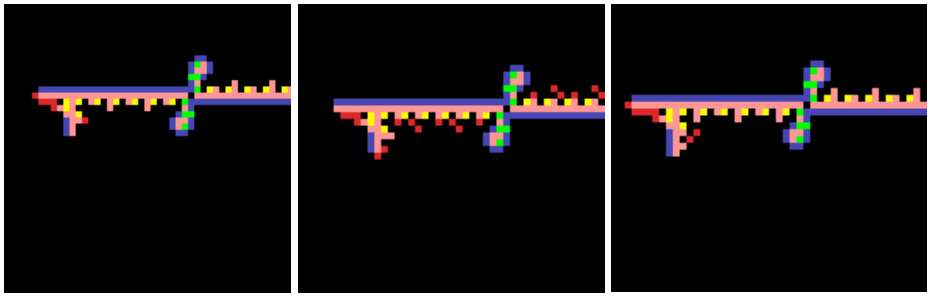

Time = 63 Time = 64 Time = 65

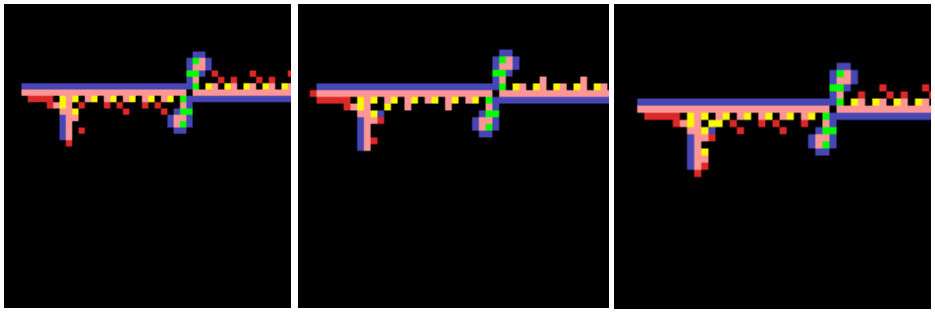

Time = 66 Time = 67 Time = 68

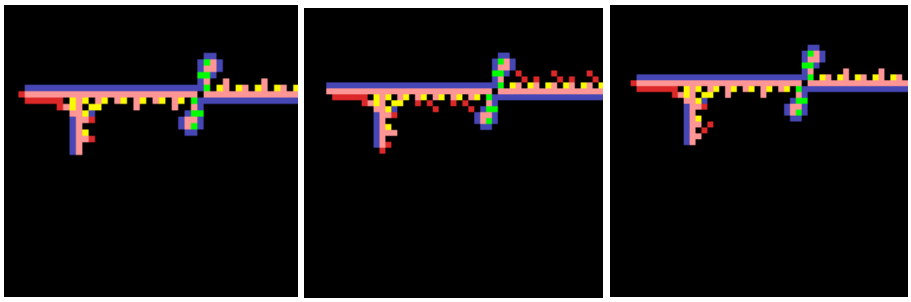

Time = 69 Time = 70 Time = 71 …

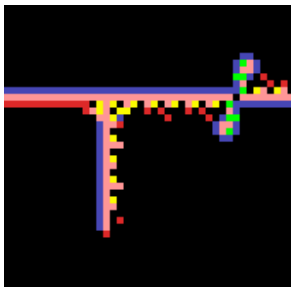

… Time = 90

Figure 4. A period-4 oscillator initiated from a single isolated cell in state 3 (pink) situated in the path of an extending arm initiated from the interaction of two replicator instances causes the arm to continue west as a band of three static states (Type **B**, see text), as the preceding arm (Type **A**) is simultaneously redirected 90^{o} to continue south. By Time = 90, the perpendicular arms have extended considerable distances.

Figure 4 above illustrates that there is more than one type of extending arms. Observations have revealed three types **A**, **B** and **C**:

A. A composite arm of two static-state layers (blue and pink, representing states 2 and 3 respectively) parallel with an adjoining oscillating layer. The Time = 50 panel of Figure 3 shows the type **A** arms extended for some distance both east and west, initiated by the interaction of two replicator instances.

B. An arm consisting of three static-state layers (blue, pink and red, representing states 2, 3 and 1 respectively). Figure 4 shows a Type **A** arm transformed to a Type **B** arm by interaction with an oscillating structure. The Time = 90 panel of Figure 4 shows the unimpeded Type **B** arm extending west for some distance after the interaction. Note simultaneous redirection south of the untransformed Type **A** arm.

C. The Type **C** arm consists of two adjoined oscillating layers. Figure 5 shows a Type **C** arm extending north, generated from the interaction of two Type **A** arms. A history culminating in the interaction is shown in Figure 8 within the section titled "Formation of compartments from a minimal arrangement of isolated active states" (page 9).

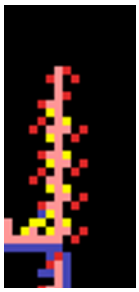

Figure 5. A Type **C** arm extending north (upwards). The developmental history from which this is extracted is detailed in Figures 8 and 9 and accompanying text.

Another structure influencing direction and/or transformation of an extending arm

The persisting and static CNESW = L2222 "cross" structure immediately emergent from CNESW = L0000 (isolated state L cell) has two functions depending on spatial placement: turning an advancing arm by 90^{o} with type transformation, or transforming an arm type without redirection. Figure 6 shows that interaction of the cross with a Type **C** arm turns its direction 90^{o} and transforms it to Type **A**. Figure 7 shows that interaction of the cross with a Type **A** arm transforms it to a Type **B** arm without changing the direction of subsequent propagation. Note the chirality of the **A** and **B** arms: in the direction of extension, the blue (state 2) layer is rightmost in both.

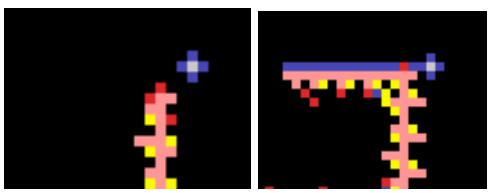

Figure 6. Left: A Type **C** arm approaching a CNESW = L2222 cross to the right of its northward direction of extension. The subsequent interaction causes the arm to turn 90^{o} left. Right: Simultaneously with the redirection, the arm is transformed to the Type **A** form, shown here after considerable extension following the interaction.

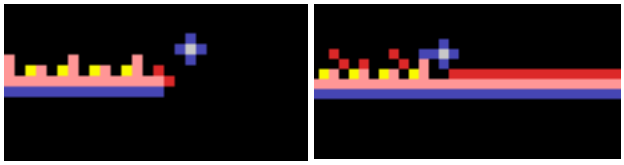

Figure 7. Left: A Type **A** arm approaching a CNESW = L2222 cross north of its eastward direction of extension. Right: At the interaction, the arm is transformed to the Type **B** form, shown here after considerable extension following the interaction. Note that direction of propagation is not affected.

Formation of compartments from a minimal arrangement of isolated active states

Figure 8 shows the formation of a compartment which eventually confines the development of an isolated replicator. At Time = 0 the two top-left (north-west) active states are F with **^** below. The two states at the south-east corner are the same configuration but rotated by 180^{o} relative to the north-west pair. The state of the cell at the centre is **^** which subsequently develops normally into a replicator instance. The neighbourhoods of the isolated F states (CNESW = F0000) at Time 0 become CNESW = FEEEE neighbourhoods at Time = 1, visible as static white crosses at north-west and south-east locations.

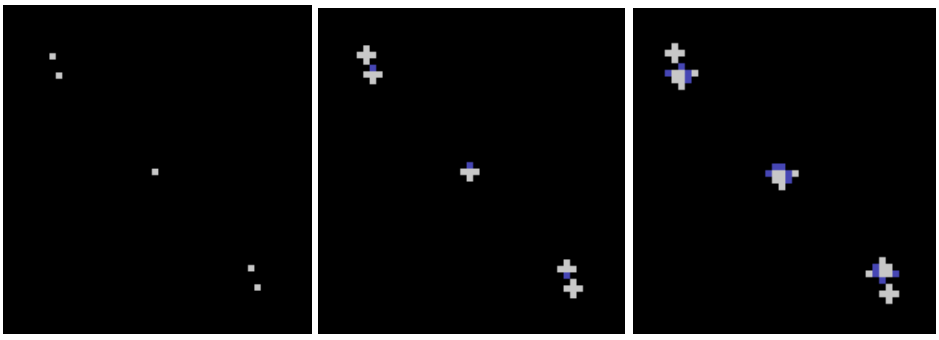

Time = 0 Time = 1 Time = 2

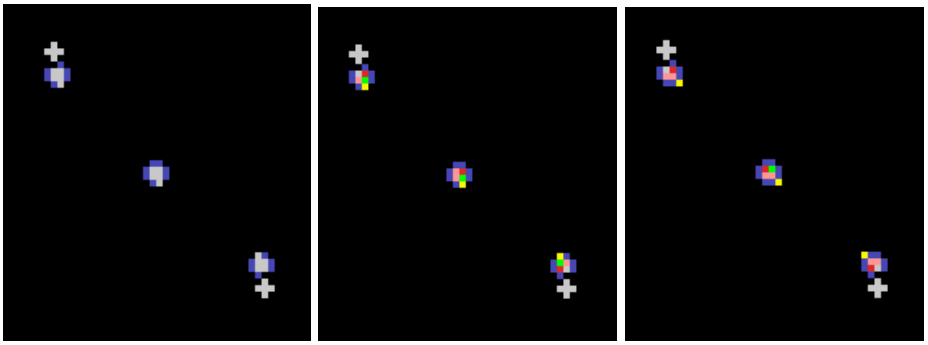

Time = 3 Time = 4 Time = 5

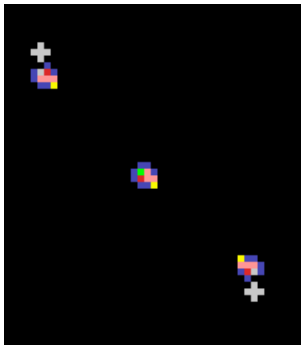

Time = 6

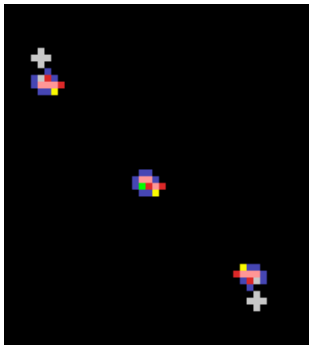

Time = 7

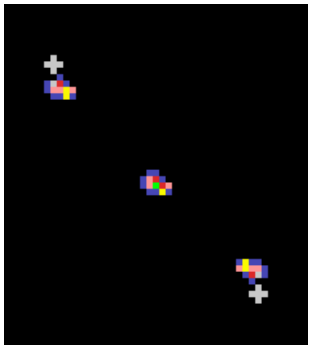

Time = 8

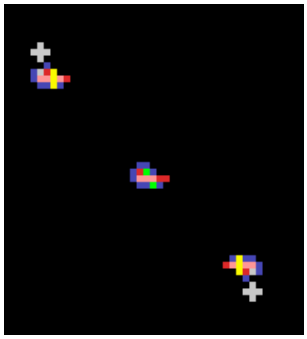

Time = 9

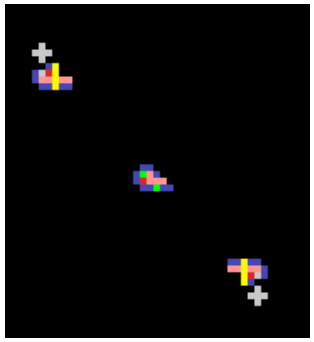

Time = 10

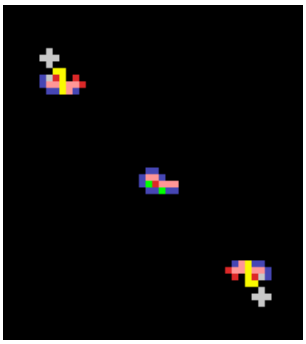

Time = 11

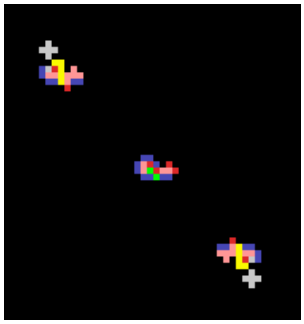

Time = 12

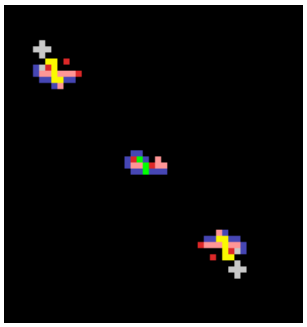

Time = 13

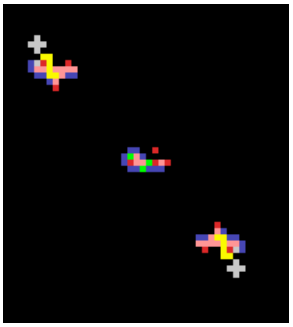

Time = 14

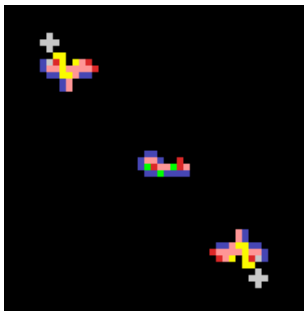

Time = 15

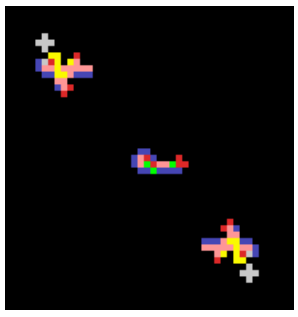

Time = 16

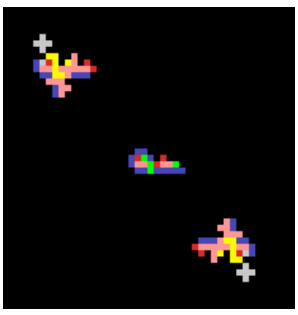

Time = 17

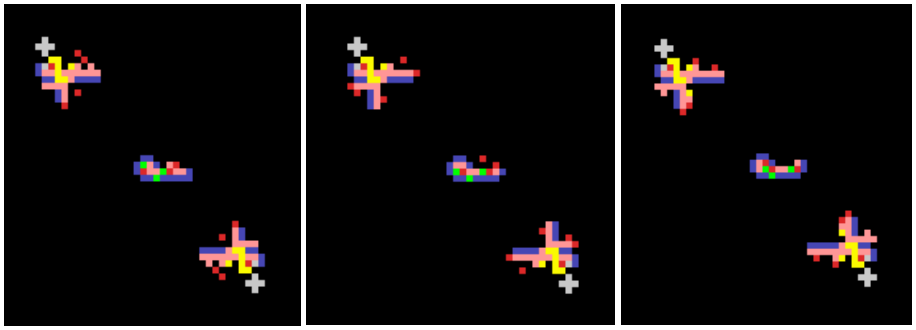

Time = 18 Time = 19 Time = 20

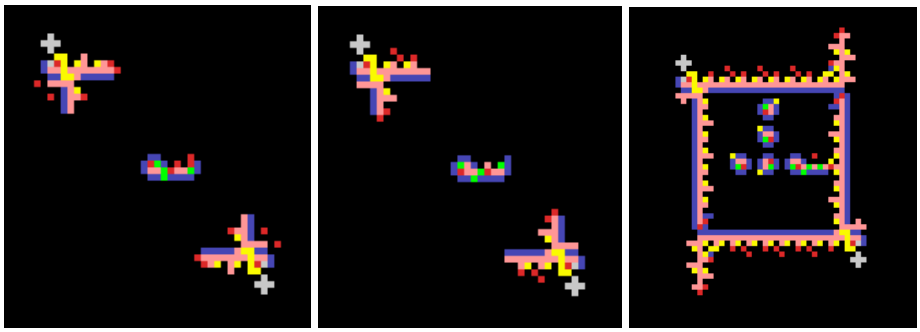

Time = 21 Time = 22 … … Time = 80

Figure 8. Formation of a quadrilateral compartment from a minimal distribution of active states at Time = 0 (see text). The compartment encloses and restricts expansion of a replicator colony inside.

At Time = 3, development of the north-west **^** state and south-east **v** state has already diverged from the normal course of forming replicator instances due to interaction with the adjacent CNESW = FEEEE cross structures. Each interaction initiates extension of two perpendicular Type **A** arms which eventually achieve closure at north-east and south-west locations defining a quadrilateral enclosure shown completed at Time = 80. The interaction at each of the north-east and south-west locations facilitates extension of a Type **C** arm north from the north-east location and south from the south-west location, and at completion of enclosure, the development of the Time = 0 **^** state at the centre has become isolated from the external environment, so unconstrained development of a subsequent replicator colony is blocked. With no impediments to extension of the Type **C** arms they can extend north and south indefinitely as illustrated in Figure 9 below showing the northward arm extending by one cell each two successive time steps. Note that the type **C** arm incorporates two adjoined oscillating layers, so the chirality of the interacting type **A** arms is not inherited.

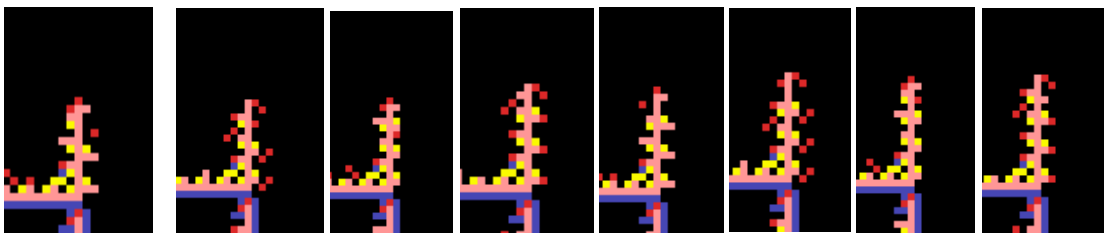

Time = 84 (12) 85 (12) 86 (13) 87 (13) 88 (14) 89 (14) 90 (15) 91 (15)

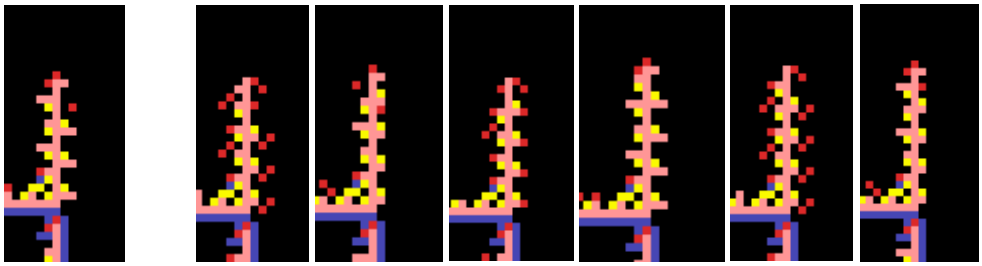

Time = 92 (16) 93 (16) 94 (17) 95 (17) 96 (18) 97 (18) 98 (19)

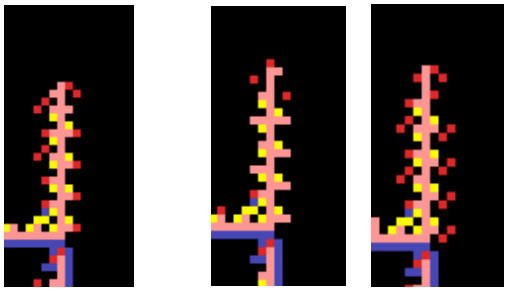

Time = 99 (19) 100 (20) 101 (20)

Figure 9. Extension of the Type **C** arm from the northeast corner of the compartment shown in Figure 8, in single time-step increments from Time = 84 to 101. The bracketed value with each time label is the length of the arm in active-state cells counted from the southernmost state 5 (yellow) cell, so the arm can be seen to extend in length by one cell each two time-steps.

At-a-glance inspection of Figure 9 does not immediately show the advance of the arm structure, as small scale-variation from one frame to another occurs due to my somewhat inexpert cropping from larger screenshots. However, the incremental advance of the arm is easily recognised by counting active cells in the direction of extension.

A compartment can be formed without the subsequent advance of the emergent Type **C** arms by the presence of simple barriers precisely placed in their paths as shown in Figure 10. At Time = 0 two persisting pairs of adjoining blue (state 2) cells are precisely placed to block the Type **C** arms generated by later completion of the compartment. The sequence of frames from Time = 80 to 84 show that the barriers are effective in permanently blocking extension of the arms so that the compartment displays no further development beyond its completion. (As an aside, note the temporal oscillation of the compartment walls.)

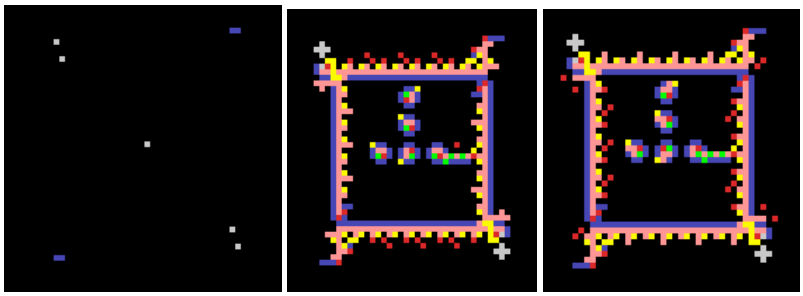

Time = 0 … … Time = 80 Time = 81

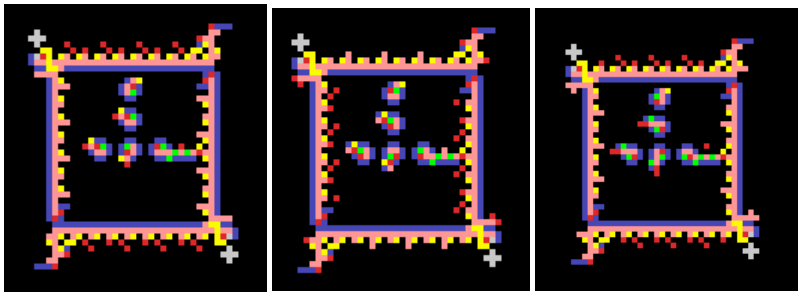

Time = 82 Time = 83 Time = 84

Figure 10. Precisely-placed barriers at north-east and south-west locations (pairs of adjoined cells in state 2, represented in blue) block the extension of Type **C** arms generated at completion of the compartment so that it completes without ongoing development. The replicator activity confined within the compartment is spatially restricted by the compartment walls.

Discussion

While we might consider that life is recognisable when we see it, a rigorous and comprehensive definition of life is surprisingly difficult to establish. It may be more meaningful to consider life as a continuum from unambiguously non-living to unambiguously living, including prions, viruses *etc.* along its range, *i.e.* a sharp threshold dividing life from non-life might not exist. With this caveat in mind, Tibor Gánti's chemical automaton (abbr. *chemoton*) [2] is the outcome of a rigorous abstraction of life intended as a universal definition of immediate interest to abiogenesis and astrobiology research. Briefly, the chemoton is a system of three stoichiometrically-synchronised automata: autocatalytic metabolic networks (cytoplasmic metabolic activity), compartmentalisation (self-assembling membranes), and information storage and transformation (production of macromolecules). In recognising life as chemical, it follows that cell physiology is *fluid*.

How does the observed spatial and temporal determinism of many life processes emerge from the stochasticity of fluid automata? As explanation, Mondal and Kolomeisky describe the "stochastic coupling method" [4] with two examples of precise cellular regulation emerging from interacting stochastic processes. Their first example describes coupling of bacterial cell growth and cell division which delivers an optimum narrow cell size distribution. The second example describes cell lysis dynamics following viral infection of bacteria. Stochastic coupling of synthesis and removal of holin proteins achieves the narrow distribution of cell lysis times optimal for release of viral copies.

Comparison of CA dynamics with fluid automata dynamics

The rigidity of fully-deterministic discrete time and space CA abstraction on a fixed grid is the antithesis of stochastic fluid automata, which indicates some limitations on what can be understood about life from CA work (though lattice-gas CA incorporate some stochasticity). Although the dynamics described in this paper were first identified from developments within a grid initialised with a stochastic distribution of cell states, the phenomena could only be reliably reproduced for further study with careful spatial alignment of cell states. However, some discussion of what CA abstraction might reveal about life is justifiable.

Life includes compartmentalisation, metabolism, and storage and implementation of information, so a problem is how these definitive requirements [2] appeared and synchronised during abiogenesis. Perhaps one specific ancestral function diversified into the suite of three requirements. The work

described in this paper shows that emergent compartmentalisation and perhaps metabolism can be supported solely by a logic of self-replication. The range of phenomena other than replication identified includes initiation of extending arms (Figure 3) and their termination (Figure 10), two-way splitting of arms (Figure 4), perpendicular redirection of arms (Figures 3 and 6), arm type transformations (Figure 7) and development of compartments (Figure 8) which are all facilitated by dynamic interactions between replicator instances and neighbouring static, oscillating and dynamically extending structures. It is also notable that this diverse range of phenomena can develop from initial arrangements of only a few active cell states. Beyond the logic of replication, the only further requirement supporting this range of phenomena is the straightforward addition of state preservation rules (CNESW → C´ = C) applying to all cell state neighbourhoods not represented in the rules explicit for replication.

The enclosure of active states within a compartment suggests the possibility of CA analogies of proto-metabolism isolated from external environments, but the rigid compartment wall (Figure 8) is a poor analogy to a cell membrane. Further explorations may discover interactions which modify compartment walls to capture the semi-permeability of biological membranes.

Interactions between internal dynamics and compartment walls could conceivably influence the dynamics toward processes recognisable as metabolism. Figure 10 shows an enclosed replication process altered by interactions with the constraining compartment wall, but the dynamic is not of a sophistication recognisable as representing a metabolism. Perhaps a larger compartment enclosing a larger distribution of states could deliver a satisfying model of a metabolism developing in isolation from the external environment.

References

[1] J Byl, Self-reproduction in small cellular automata, *Physica D* **34** (1989) 295-299.

[2] T Gánti, *The Principles of Life*, Oxford University Press (2003) 201 pp.

[3] CG Langton, Self -reproduction in cellular automata, *Physica D* **10** (1984) 135-144.

[4] A Mondal and AB Kolomeisky, Microscopic origin of the spatial and temporal precision in biological systems, *Biophysical Reports* **5** (2025) 1-12.

[5] C Reas and B Fry, *Processing, A Programming Handbook for Visual Designers and Artists* (second edition). MIT Press, Cambridge MA (2014) 662 pp.

[6] PW Swanborough, Development of a Two-Dimensional Replicator from a Single Non-Quiescent Cell in Cellular Automata Space. *viXra:2201.0025* (2022).

[7] PW Swanborough, Macroscopic Structures Emerging from the Interactions of Simple Replicators. *viXra:2501.0072* (2025).